

COMMUNICATION

This is a peer reviewed version of the following article: Phys. Chem. Chem. Phys. 2016, 18, 32668, which has been published in final form at <http://pubs.rsc.org/en/content/articlelanding/2016/cp/c6cp06799a#!divAbstract>

Rationalizing Fluorescence Quenching in *meso*-BODIPY Dyes

Antonio Prlj,^{a†} Alberto Fabrizio^{a†} and Clemence Corminboeuf^{a*}

Received 00th January 20xx,

Accepted 00th January 20xx

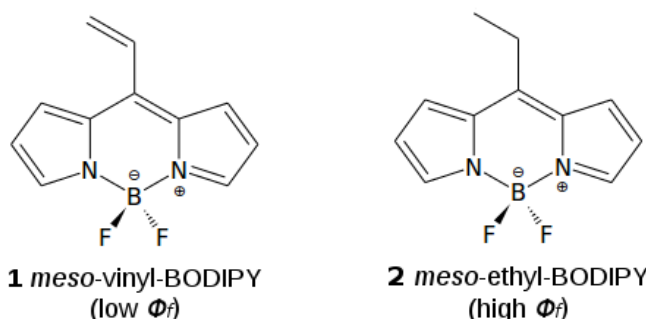
DOI: 10.1039/x0xx00000x

www.rsc.org/

Meso-substituted boron-dipyrromethene (BODIPY) dyes are a puzzling class of molecules, which feature contrasting emissive behaviors. The full mechanistic picture for these distinctive properties is still missing. Using static and dynamic excited state computations we unravel the key reasons behind these divergences.

Boron-dipyrromethene (BODIPY) dyes are one foremost class of small organic molecules with wide applications in imaging and sensing,¹ photovoltaics,² electrochemistry,³ non-linear optics,⁴ lasers⁵ etc. Key features of these compounds include excellent thermal and chemical stability as well as sharp absorption and emission bands with fluorescence quantum yields approaching 100%.⁶ Their optoelectronic properties are generally tunable by introducing various substituents, which has prompted extensive synthetic efforts and fine-tuning of their optical performance through both experimental⁷ and quantum-chemical modelling.⁸ Owing to its unique versatility,⁹ the BODIPY dye was labeled as the “El Dorado for fluorescence tools”^{9a} and “the most versatile fluorophore ever”.^{9b} However, *a priori* knowledge of the structure-property relationships connecting the substituent and the emissive property of the dye still remains the holy grail for molecular design. *Meso*-substituted BODIPYs received special attention due to their evident contrasting emissive behaviors.^{10,11} Small variations in the nature of the substituents are associated with dramatically different photophysical properties. In particular, BODIPY is strongly

fluorescent upon UV irradiation if bonded to a sp^3 carbon, whereas the fluorescence of the sp^2 -bonded analogue is almost completely quenched.¹¹ In particular, the excellent fluorescence characteristics of the parent BODIPY are preserved in the *meso*-substituted alkyl chains core (fluorescence quantum yields, $\Phi_f > 0.9$)^{10c,11a,12} but the *meso*-alkenyl derivatives are virtually non-fluorescent ($\Phi_f \approx 0$).^{11a,12,13} Cosa *et al.* have shown that the same contrast holds for formyl (sp^2 , non-fluorescent) and hydroxymethyl (sp^3 , fluorescent), or iminyl (sp^2 , non-fluorescent) and aminomethyl (sp^3 , fluorescent) moieties.^{11b} Such sharp differences in emissive properties do not typically hold for α - and β -substituted derivatives (see ref. 13 and the examples therein). The full mechanistic picture of the nonradiative decay in *meso*-substituted dyes is still missing even though the quantum yield drop was attributed to intramolecular deactivation pathways, consistent with the large Stokes shifts, rather than to a quenching mechanism such as intersystem crossing.^{11b} In this contribution, we unravel the key physical reasons



behind the different emissive properties of two exemplary compounds *meso*-vinyl and *meso*-ethyl BODIPY (Scheme 1).

Scheme 1. Schematic 2D representations of the studied compounds with their expected fluorescence quantum yields (Φ_f).

^a Institut des Sciences et Ingenierie Chimiques, Ecole Polytechnique Federale de Lausanne, CH-1015 Lausanne, Switzerland. E-mail: clemence.corminboeuf@epfl.ch

[†] Authors contributed equally.

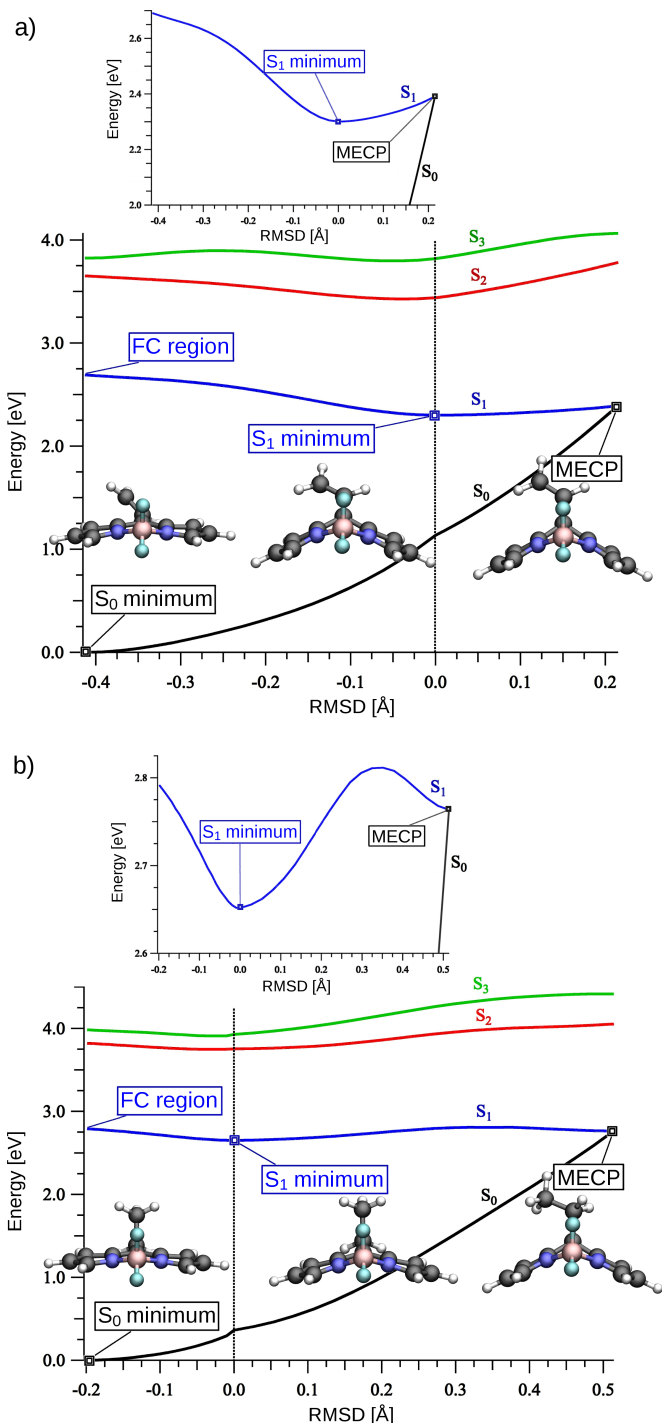
Electronic Supplementary Information (ESI) available: details of any supplementary information available should be included here. See DOI: 10.1039/x0xx00000x

Relying upon high level excited state and molecular dynamics computations, we provide evidences that **1** is more likely to deactivate non-radiatively from the first excited singlet state (S_1) to the ground state (S_0) due to the accessible conical intersection (CI). CIs are crossings between potential energy surfaces (of the same multiplicity), which enable very efficient non-radiative decay¹⁴ and proved to be important to explain fluorescence properties of many organic dyes.¹⁵ In principle, a CI may be separated from the Franck-Condon (FC) region and the excited state minimum by a potential energy barrier. If the barrier can be easily overcome, the crossing region is energetically accessible and the system will easily undergo radiationless decay to the ground state. In contrast, large barriers will suppress the radiationless deactivation and promote fluorescence.

Figure 1. Energy profiles (in eV) of a) **1** and b) **2**. Optimized structures are shown as insets, while intermediate structures are obtained by linear interpolation of internal coordinates. Zoom into the S_1 topography is shown in smaller graphs. "MECP" stands for minimal energy crossing point. The ADC(2)/MP2 levels were used with the def2-SVP basis set.

The electronic state profiles using a reaction coordinate that characterizes the excited state decay are provided in Figure 1 for both **1** and **2**. The geometry deformation largely corresponds to the butterfly-like motion of the BODIPY core, bending over the boron-meso-C line. Upon this geometrical change, the excited state potential energy surfaces are clearly flatter than that of the ground state. The key difference is revealed by a closer look at the energy landscape of the first excited state. The initial excitation of **1** to the S_1 state is followed by the large energetic relaxation (~ 0.4 eV) to the S_1 minimum, associated with the puckering of the BODIPY ring. The S_1/S_0 crossing point is geometrically close to the S_1 minimum, so the small geometrical evolution prompts the non-radiative relaxation to the ground state. The situation for **2** is rather different. As opposed to **1**, for which the excitation can delocalize to the π -system of the vinyl substituent (having a weak charge transfer character; see Figure S1 in the SI), the relaxation effects in **2** are modest (~ 0.15 eV). The S_1 minimum is geometrically distant from the crossing, which is separated by an energy barrier. While the crossing is at a slightly lower energy than the FC point, the whole process following the reaction coordinate is energetically unfavorable. Hence the retention of the system close to the S_1 minimum prompts the radiative decay (*i.e.*, fluorescence). Additionally, the oscillator strength (between S_1 and S_0) in the excited state minimum is almost three times larger for **2** (0.29) than for **1** (0.11), which goes along with the smaller geometrical distortion of the former and points to its larger tendency for radiative decay. Nevertheless, the static profiles displayed in Figure 1 are not without deficiencies. In fact, the molecule absorbs a broad range of frequencies, which requires the sampling of various ground state geometries. Photoexcited molecules have already acquired a certain kinetic energy, which may help overcoming the potential barrier (note that the interpolated barrier in Figure 1b is only the upper bound for the true barrier). Additionally, the crossings are typically reached at the higher energies rather than the minimal energy crossing point.¹⁶ It is therefore not clear as whether the intersection region is also energetically accessible to **2**. Finally, alternative pathways and the possible participation of the higher excited states (through nonadiabatic coupling) are disregarded in this static picture (Figure 1).

To overcome these limitations, we provide more realistic molecular dynamic computations by initiating 50 independent trajectories in the S_1 states of both molecules. Initial conditions (*i.e.* structures and velocities) were sampled from the Boltzmann ensemble at 300K and vertical excitations from the ground state equilibrium to the non-equilibrium S_1 state were assumed. In line with the static picture, all 50 trajectories of **1** follow the butterfly-like motion and reach the crossing intersection with S_0 . In sharp contrast, only one out of 50 computed trajectories of **2** reaches the crossing within the 1ps



simulation time. The results confirm the behavior anticipated from the much simpler profiles of Figure 1: **1** shows a large tendency for radiationless decay, whereas due to the energy barrier and the longer timescales involved, **2** tends to favor fluorescence.

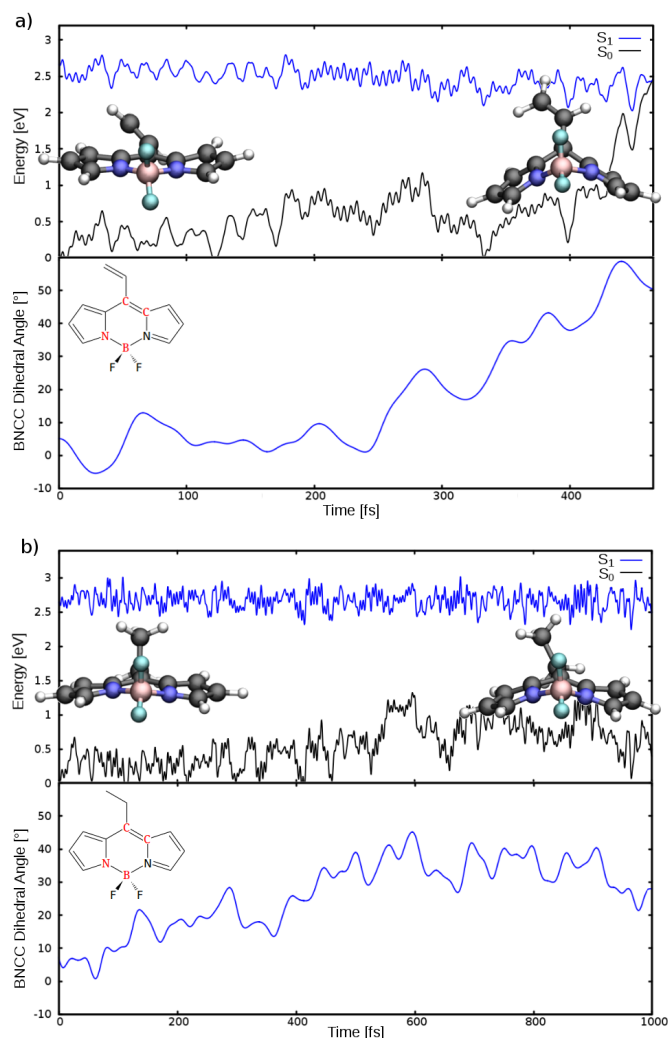


Figure 2. Illustrative trajectories for the S_1 dynamics of a) **1** and b) **2**, showing the time evolution of the potential energy surfaces of the ground and first excited states, as well as BNCC torsional angle (atoms in red). Geometries of the first and the last frame of the dynamics are depicted. ADC(2)/MP2/def2-SVP levels were used.

The excited state molecular dynamics simulation also confirms that there is no participation from the higher excited states, as can be anticipated from the relatively large energy gaps between S_1 and S_2 . Exemplary trajectories of both **1** and **2** are depicted in Figure 2, showing the time evolution of the electronic state potential energies and the simultaneous bending of the BODIPY core. While **1** evolves towards the S_1/S_0 intersection with the progressive bending of the fused core, **2** relaxes to the excited state minimum as indicated by the oscillations of the puckering angle.

Considering the ensemble of trajectories, the computed lower bound for the S_1 lifetime of **1** (in vacuum) is roughly 0.6 ps, while the S_1 lifetime of **2** is inconclusive. Nevertheless, the solvent is expected to further slow down the relevant low-frequency motions, extending the timescales to the picosecond time range. We thus recomputed the potential energy surfaces (as in Figure 1) including the implicit tetrahydrofuran (THF; used in experiments^{11a}) solvent (see SI), which shows no qualitative difference when compared to the vacuum case. Excited state molecular dynamics with explicit THF solvent (within the QM-MM framework) were also performed (see SI). In this case, none of the trajectories reached the crossing within the imposed simulation time of 1 ps. The static and the dynamic pictures indicate that the solvent does not alter the photophysics of these compounds, apart from slowing down the dynamics due to the solvent drag. While desirable, the consideration of longer timescales is unfortunately cumbersome for real time molecular dynamics computations.

To summarize, the divergence in fluorescence properties of two BODIPY dyes stems from the different topography of the S_1 potential energy surface. **1** exhibits large stabilization upon photoexcitation along with the bending of the fused BODIPY core. The crossing with the ground state is close to the excited state minimum so the population quickly decays to S_0 . **2** is qualitatively different. Excited state relaxation is modest and the crossing with the ground state is geometrically and energetically distant, due to the presence of a kinetic barrier. This difference points towards a dominant radiative relaxation pathway. From the general perspective of the fluorescence in BODIPY derivatives, the importance of Cl (and its accessibility) still has to be investigated as theoretical studies on this topic are scarce.^{12,17} Previous explanations of non-radiative decay involving concepts such as intramolecular charge transfer and the lack of molecular rigidity^{13,10b} are somewhat too general. The vast experimental work^{10,11} on *meso*-BODIPY dyes indicates that the principles demonstrated here have broader significance. In fact, we have verified that *meso*-formyl and *meso*-hydroxymethyl derivatives are qualitatively similar to **1** and **2**, respectively (see SI). Therefore, we expect that the computational modeling will be of great relevance as a future guide for rational design.

We acknowledge the funding from the Swiss National Science Foundation (no. 156001) and the European Research Council (ERC Grants 306528, "COMPOREL"). The authors thank Dr. Momir Mališ and Dr. Basile Curchod for discussions, and Dr. Ganna Gryn'ova for graphical support.

Computational Section

Excited states were computed at the ADC(2) level¹⁸ combined with the def2-SVP¹⁹ basis set. The resolution of identity and frozen core approximations were employed. ADC(2) has proved to be reliable for potential energy surfaces^{20,15c} and excited state dynamics²¹ of organic molecules. The method is particularly applicable for BODIPY dyes owing to the importance of differential correlation effects (which limits the use of standardly employed excited state methods such as TDDFT and CASSCF).²² Single point computations and optimizations were performed with Turbomole 6.5 software.²³ Minimal energy crossing points were optimized using CIOpt code²⁴

coupled to Turbomole. Although ADC(2) does not provide the correct 2D branching space of the conical intersection between the first excited and the ground state (computed at MP2 level), but rather 1D diabatic-like crossing, detailed benchmark study²⁵ has shown that it can provide correct geometries and energetics of the crossing, motivating the use of ADC(2) for photochemistry. Nevertheless, we here focus on the qualitative picture, while more quantitative data are provided in the supporting information. Molecular geometries between the optimized structures were obtained by the linear interpolation of internal coordinates, while the relative length of the paths (Figure 1) were scaled based on the root mean square deviation (RMSD) between the first and the last structure. Ground and excited state dynamics was performed with the Newton-X software²⁶ coupled to Turbomole. To sample the

initial conditions, 20 ps long ground state dynamic trajectories were performed for both systems within the NVT ensemble at 300K (Anderson thermostat). The PBE0²⁷/def2-SVP level was employed, with the time step of 1 fs. 50 initial conditions (coordinates and velocities) were sampled randomly from the last 15 ps of dynamics, and used for excited state dynamics initiated from S₁. 50 trajectories (of each compound) were evolved within the NVE ensemble with the time step of 0.5 fs and the maximal time of 1 ps. Two higher excited state were included via the surface hopping scheme,²⁸ but since there was virtually no population of these states, the dynamics is equivalent to an adiabatic dynamics in S₁. All the trajectories were terminated when approaching to the crossing with the ground state, as discussed earlier.^{21a} For further details see supporting information.

Notes and references

- 1 N. Boens, V. Leen and W. Dehaen, *Chem. Soc. Rev.*, 2012, **41**, 1130.
- 2 (a) S. Kolemen, Y. Cakmak, S. Erten-Ela, Y. Altay, J. Brendel, M. Thelakkat and E. U. Akkaya, *Org. Lett.*, 2010, **12**, 3812; (b) S. Kolemen, O. Altan Bozdemir, Y. Cakmak, G. Barin, S. Erten-Ela, M. Marszalek, J. Yum, S. M. Zakeeruddin, M. K. Nazeeruddin, M. Grätzel and E. U. Akkaya, *Chem. Sci.*, 2011, **2**, 949.
- 3 A. B. Nepomnyashchii and A. J. Bard, *Acc. Chem. Res.*, 2012, **45**, 1844.
- 4 (a) W. Shi, P. Lo, A. Singh, I. Ledoux-Rak and D. K. P. Ng, *Tetrahedron*, 2012, **68**, 8712; (b) G. Ulrich, A. Barsella, A. Boeglin, S. Niu and R. Ziessel, *ChemPhysChem*, 2014, **15**, 2693.
- 5 (a) K. K. Jagtap, N. Shivran, S. Mula, D. B. Naik, S. K. Sarkar, T. Mukherjee, D. K. Maity and A. K. Ray, *Chem. Eur. J.*, 2013, **19**, 702; (b) G. Duran-Sampedro, I. Esnal, A. R. Agarrabeitia, J. Bañuelos Prieto, L. Cerdán, I. García-Moreno, A. Costela, I. Lopez-Arbeloa and M. J. Ortiz, *Chem. Eur. J.*, 2014, **20**, 2646.
- 6 G. Ulrich, R. Ziessel and A. Harriman, *Angew. Chem. Int. Ed.*, 2008, **47**, 1184.
- 7 (a) K. Umezawa, A. Matsui, Y. Nakamura, D. Citterio and K. Suzuki, *Chem. Eur. J.*, 2009, **15**, 1096; (b) W. Wu, H. Guo, W. Wu, S. Ji and J. Zhao, *J. Org. Chem.*, 2011, **76**, 7056; (c) A. B. Nepomnyashchii, M. Bröring, J. Ahrens and A. J. Bard, *J. Am. Chem. Soc.*, 2011, **133**, 8633; (d) D. K. Kölmel, A. Hörner, J. A. Castañeda, J. A. P. Ferencz, A. Bihlmeier, M. Nieger, S. Bräse and L. A. Padilha, *J. Phys. Chem. C*, 2016, **120**, 4538; (e) M. Saikawa, T. Nakamura, J. Uchida, M. Yamamura and T. Nabeshima, *Chem. Commun.*, 2016, **52**, 10727.
- 8 (a) S. Chibani, B. Le Guennic, A. Charaf-Eddin, A. D. Laurent and D. Jacquemin, *Chem. Sci.*, 2013, **4**, 1950; (b) B. Le Guennic, O. Maury and D. Jacquemin, *Phys. Chem. Chem. Phys.*, 2012, **14**, 157; (c) M. R. Momeni and A. Brown, *J. Phys. Chem. A*, 2016, **120**, 2550; (d) X. Liu, J. Zhang, K. Li, X. Sun, Z. Wu, A. Ren and J. Feng, *Phys. Chem. Chem. Phys.*, 2013, **15**, 4666; (e) S. Mukherjee and P. Thilagar, *RSC Adv.*, 2015, **5**, 2706; (f) J. Wang, J. Jin, Y. Geng, S. Sun, H. Xu, Y. Lu and Z. Su, *J. Comput. Chem.*, 2013, **34**, 566.
- 9 (a) R. Ziessel, G. Ulrich and A. Harriman, *New. J. Chem.*, 2007, **31**, 496; (b) J. Bañuelos, *Chem. Rec.*, 2016, **16**, 335.
- 10 (a) H. L. Kee, C. Kirmaier, L. Yu, P. Thamyongkit, W. J. Youngblood, M. E. Calder, L. Ramos, B. C. Noll, D. F. Bocian, W. R. Scheidt, R. R. Birge, J. S. Lindsey and D. Holten, *J. Phys. Chem. B*, 2005, **109**, 20433; (b) R. Hu, E. Lager, A. Aguilar-Aguilar, J. Liu, J. W. Y. Lam, H. H. Y. Sung, I. D. Williams, Y. Zhong, K. S. Wong, E. Peña-Cabrera and B. Z. Tang, *J. Phys. Chem. C*, 2009, **113**, 15845; (c) J. Bañuelos, I. J. Arroyo-Córdoba, I. Valois-Escamilla, A. Alvarez-Hernández, E. Peña-Cabrera, R. Hu, B. Z. Tang, I. Esnal, V. Martínez and I. L. Arbeloa, *RSC Adv.*, 2011, **1**, 677; (d) A. A. Pakhomov, Y. N. Kononevich, A. A. Korlyukov, V. I. Martynov and A. M. Muzafarov, *Mendeleev. Commun.*, 2016, **26**, 196.
- 11 (a) I. J. Arroyo, R. Hu, B. Z. Tang, F. I. López and E. Peña-Cabrera, *Tetrahedron*, 2011, **67**, 7244; (b) R. Lincoln, L. E. Greene, C. Bain, J. O. Flores-Rizo, D. S. Bohle and G. Cosa, *J. Phys. Chem. B*, 2015, **119**, 4758; (c) K. Krumova, G. Cosa, *J. Am. Chem. Soc.*, 2010, **132**, 17560.
- 12 L. Jiao, C. Yu, J. Wang, E. A. Briggs, N. A. Besley, D. Robinson, M. J. Ruedas-Rama, A. Orte, L. Crovetto, E. M. Talavera, J. M. Alvarez-Pez, M. Van der Auweraer and N. Boens, *RSC Adv.*, 2015, **5**, 89375.
- 13 H. Lu, J. Mack, Y. Yang and Z. Shen, *Chem. Soc. Rev.*, 2014, **43**, 4778.
- 14 (a) J. Michl and V. Bonačić-Koutecký, *Electronic Aspects of Organic Photochemistry*, Wiley-Interscience, 1990; (b) W. Domcke, D. R. Yarkony and H. Köppel, *Conical Intersections – Theory, Computation and Experiment*, World Scientific, Singapore, 2011. (c) G. J. Atchity, S. S. Xantheas and K. Ruedenberg, *J. Chem. Phys.*, 1991, **95**, 1862; (d) S. Matsika and P. Krause, *Annu. Rev. Phys. Chem.*, 2011, **62**, 621; (e) D. R. Yarkony, *Chem. Rev.*, 2012, **112**, 481; (f) W. Domcke and D. R. Yarkony, *Annu. Rev. Phys. Chem.*, 2012, **63**, 325.
- 15 (a) Q. Li and L. Blancafort, *Chem. Commun.*, 2013, **49**, 5966; (b) Y. Harabuchi, T. Taketsugu and S. Maeda, *Phys. Chem. Chem. Phys.*, 2015, **17**, 22561; (c) M. Barbatti and H. Lischka, *Phys. Chem. Chem. Phys.*, 2015, **17**, 15452; (d) J. Brazard, L. A. Bizimana, T. Gellen, W. P. Carbery and D. B. Turner, *J. Phys. Chem. Lett.*, 2016, **7**, 14; (e) A. Prlj, N. Došlić and C. Corminboeuf, *Phys. Chem. Chem. Phys.*, 2016, **18**, 11606.
- 16 L. Blancafort, *ChemPhysChem*, 2014, **15**, 3166.
- 17 M. Buyuktemiz, S. Duman and Y. Dede, *J. Phys. Chem. A*, 2013, **117**, 1665.
- 18 (a) A. B. Trofimov and J. Schirmer, *J. Phys. B: At. Mol. Opt. Phys.*, 1995, **28**, 2299; (b) A. Dreuw and M. Wormit, *WIREs Comput. Mol. Sci.*, 2015, **5**, 82.
- 19 (a) F. Weigend and R. Ahlrichs, *Phys. Chem. Chem. Phys.*, 2005, **7**, 3297; (b) F. Weigend, *Phys. Chem. Chem. Phys.*, 2006, **8**, 1057.
- 20 (a) D. Tuna, A. L. Sobolewski and W. Domcke, *J. Phys. Chem. A*, 2014, **118**, 122; (b) A. Prlj, B. F. E. Curchod, A. Fabrizio, L. Floryan and C. Corminboeuf, *J. Phys. Chem. Lett.*, 2015, **6**, 13; (c) X. Liu, T. N. V. Karsili, A. L. Sobolewski and W. Domcke, *J. Phys. Chem. B*, 2015, **119**, 10664; (d) T. N. V. Karsili, D. Tuna, J. Ehrmaier and W. Domcke, *Phys. Chem. Chem. Phys.*, 2015, **17**, 32183; (e) D. Tuna and W. Domcke, *Phys. Chem. Chem. Phys.*, 2016, **18**, 947.
- 21 (a) F. Plasser, R. Crespo-Otero, M. Pederzoli, J. Pittner, H. Lischka and M. Barbatti, *J. Chem. Theory Comput.*, 2014, **10**, 1395; (b) M. Barbatti, *J. Am. Chem. Soc.*, 2014, **136**, 10246; (c) A. Prlj, B. F. E. Curchod and C. Corminboeuf, *Phys. Chem. Chem. Phys.*, 2015, **17**, 14719; (d) M. A. Kochman, A. Tajti, C. A. Morrison and R. J. Dwayne Miller, *J. Chem. Theory Comput.*, 2015, **11**, 1118; (e) M. Sapunar, A. Ponzi, S. Chaiwongwattana, M. Mališ, A. Prlj, P. Decleva and N. Došlić, *Phys. Chem. Chem. Phys.*, 2015, **17**, 19012; (f) S. Chaiwongwattana, M. Sapunar, A. Ponzi, P. Decleva and N. Došlić, *J. Phys. Chem. A*, 2015, **119**, 10637; (g) R. Szabla, R. W. Gorá and J. Šponer, *Phys. Chem. Chem. Phys.*, 2016, **18**, 20208.
- 22 (a) A. Charaf-Eddin, B. Le Guennic and D. Jacquemin, *RSC Adv.*, 2014, **4**, 49449; (b) B. Le Guennic and D. Jacquemin, *Acc. Chem. Res.*, 2015,

- 48, 530; (c) M. R. Momeni and A. Brown, *J. Chem. Theory Comput.*, 2015, **11**, 2619.
- 23 F. Furche, R. Ahlrichs, C. Hättig, W. Klopper, M. Sierka and F. Weigend, *WIREs Comput. Mol. Sci.*, 2014, **4**, 91.
- 24 B. G. Levine, J. D. Coe and T. J. Martínez, *J. Phys. Chem. B.*, 2008, **112**, 405.
- 25 D. Tuna, D. Lefrancois, Ł. Wolański, S. Gozem, I. Schapiro, T. Andruniów, A. Dreuw and M. Olivucci, *J. Chem. Theory Comput.*, 2015, **11**, 5758.
- 26 M. Barbatti, M. Ruckebauer, F. Plasser, J. Pittner, G. Granucci, M. Persico and H. Lischka, *WIREs Comput. Mol. Sci.*, 2014, **4**, 26.
- 27 C. Adamo and V. Barone, *J. Chem. Phys.*, 1999, **110**, 6158.
- 28 J. C. Tully, *J. Chem. Phys.*, 1990, **93**, 1061.